



Key Technology of Offshore Small Buoy Deployment Based on Bayesian Network

Ji-ming Zhang^{1,2,3}(✉) and Xuan-qun Li^{1,2,3}

- ¹ Institute of Oceanographic Instrumentation, Qilu University of Technology (Shandong Academy of Sciences), Qingdao 266000, China
- ² Shandong Provincial Key Laboratory of Ocean Environmental Monitoring Technology, Qingdao 266000, China
- ³ National Engineering and Technological Research Center of Marine Monitoring Equipment, Qingdao 266000, China

Abstract. In view of the high probability of natural or man-made damage during deployment and operation of offshore small buoys, after summing up the research institute's years of experience and knowledge in the development, production and maintenance of offshore small buoys, a new method based on shellfish has been proposed. The key technology for the deployment of small buoys in the coastal waters of the Yes Networks, through the analysis of marine environmental characteristics and buoy release requirements, effectively guides the deployment and maintenance of small buoys. The popularization and application of this technology shows that this technology can improve the deployment and maintenance of small buoys. Maintain efficiency, work efficiency and operational safety.

Keywords: Bayesian network · Offshore buoy · Buoy deployment · Release demand

1 Introduction

The small multi-parameter marine environment monitoring buoy has the characteristics of small size, convenient transportation, and the ability to comprehensively measure various marine data. It is widely used in offshore waters and exerts the function of unmanned transmission of data and information [1]. But also because of its small size and light weight, its deployment location does not belong to the remote deep sea area, and the probability of various natural and man-made damages is greater. Therefore, in order to reduce the probability of damage to the small buoy, make it as long as possible. Extending, the various tasks before, during and after the deployment cannot be ignored. Since the deployment location, sea conditions, and requisitioned vessels of small buoys are different each time, we will not describe in detail the various links of the entire deployment of buoys, only the links that may affect the normal operation of the buoys after they enter the water. Put forward and provide corresponding solutions for reference [2]. At present, there are still differences in the operating environment of buoys at home

and abroad. Foreign countries generally operate fully mechanized, using large ships to load several buoys, and after reaching the designated position, they are hoisted into the sea with a ship-mounted boom. At present, only a few locations in China can adopt this method. With sufficient funds and smooth coordination, vessels with ample aft deck, hoisting booms and winches can be requisitioned; if conditions do not permit, a vessel with a wide aft deck and lower ship can be used instead, and a ship with better sea conditions can be selected. Go to sea for deployment [3]. The following are the key links that should be paid attention to in the whole process of offshore small buoys.

2 Key Technology for the Deployment of Offshore Small Buoys

2.1 Placement of Small Offshore Buoys

Since the deployment location is offshore, it is often close to the land, and there are many ships in the deployment area, and collisions may occur regardless of day and night. Therefore, the surrounding sea area should be carefully inspected before deployment, and the latitude and longitude are roughly unchanged. Make small-scale adjustments. Pay attention to choosing the sea area away from the channel port, the sea area away from the fishermen's work area, and the sea area that is more prone to marine accidents, such as sea reef areas. The reef exposed at low tide will cause serious damage to the buoy body. For example, the oil terminal, because oil leakage often occurs in the sea near the oil terminal, the leaked oil directly has a serious adverse effect on the buoy body [4]. At present, there are roughly four ways for people to obtain marine information, namely: marine monitoring buoys, satellite remote sensing, ship sailing, and coastal marine stations. Marine buoys play a huge role in the observation of marine environment and hydrological information. How to accelerate the development of buoy technology is of great significance to the development and utilization of the ocean [5]. In the overall technology of marine buoys, the buoy body as the carrier of each monitoring instrument is related to whether it can provide the required working conditions for the equipment. Therefore, the design of the buoy body structure is very important in the overall design of the buoy [6]. As a floating structure on the sea, the offshore buoy structure combines the characteristics of offshore engineering structure and floating structure. As a small offshore buoy, compared with large offshore buoys, offshore buoys are more susceptible to damage from the complex marine environment. Therefore, the structural design and research of offshore buoys is the key and difficult point in the overall design of marine buoys [7]. These four observation methods have their own advantages and disadvantages, as shown in the table (Table 1):

Marine buoy monitoring is an advanced and practical marine monitoring method. This method is developed on the basis of traditional marine monitoring methods. It can realize unmanned, automatic, fixed-point, regular and continuous monitoring of various hydrological elements at sea. The monitoring of environmental elements is one of the main tools for studying various marine physical, chemical and biological phenomena [8]. It forms a three-dimensional marine monitoring system with satellites, marine survey ships, marine surveillance aircraft, and submersibles. Compared with the other three monitoring methods, marine monitoring buoys have the advantages of mobile and flexible layout, long-term continuous, all-weather fixed-point monitoring, and are used

Table 1. Detection methods and advantages and disadvantages

Observation approach	Inferiority	Advantage
Satellite remote sensing	The accuracy of data is not high, and the types of measurable sample parameters are few	Continuous data monitoring, fast data transmission and large work coverage
Coastal marine station	Only the data of coastal marine environment can be obtained	Data continuity, high accuracy
Ocean detection buoy	It is difficult to design, launch and maintain the ocean buoy	Multifunction, continuous detection, long life, low cost, strong viability
Ship sailing	The cost of monitoring is high, and it cannot be monitored continuously for a long time	It has high measurement accuracy and many kinds of measurable parameters

by more and more countries and regions in the development of marine energy resources, marine environmental forecasting, and maritime defense construction.

Small buoys need to be transferred from land to the ocean. Generally, a crane or crane is used. It is recommended that the boom should be longer than 5t. If it is towed at sea, it should be transferred to the sea at full tide as much as possible to avoid collisions under the sea. Reef: When towing, pay attention to keeping a certain distance between the buoy and the ship to reduce the possibility of collision [9]. The towing speed is within 5 knots to prevent the target body from tipping over. If it is hoisted to the deck, ample storage space and a stable base are required. Before launching into the water, a final inspection of each key part of the seal is necessary, which has a direct relationship with the life of the instrument inside the buoy. The connection work of the anchor system is generally completed at sea, and the installation personnel must be skilled. Pay attention to the placement and fixing of the anchor and the anchor chain during the work to avoid the anchor chain from knotting or falling into the water. The specific placement depends on the hull of the ship [10]. The derrick of the underwater equipment needs to reach the sea area where it is deployed, and then install it after anchoring and stabilization, so as to avoid scraping the fishing net or submerged reef during towing. When planning the buoy search submarine formation, it is usually necessary to make the two buoys have a certain overlap [11]. The maximum allowable error of the buoy array should meet the buoy's non-missing warning coverage condition, that is, there should be no coverage gap between two buoys in the formation, so that the submarine may pass through the gap between the buoys without being detected. As shown (Fig. 1).

In the figure, Δd is the deviation distance between the actual position of the buoys and the position of the planned lattice point when the two buoys' range circles are tangent. In order to avoid missing alarms, the error Δd when the two buoys' range circles are exactly tangent is defined as the maximum delivery error. Assuming that the buoy's operating distance is 3 km and the planned buoy spacing is 4.8 km, it can be known from the geometric relationship that the maximum delivery error of the buoy without missing alarm is 600 m. In the process of random placement, the normal distribution model is

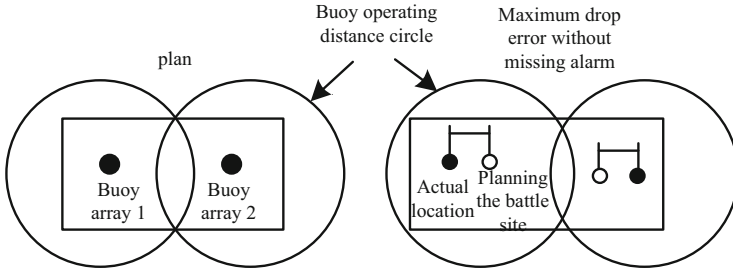


Fig. 1. Schematic of the maximum release error of the buoy formation

used to describe the error distribution, and the $\pm 3\sigma$ range is required to be $(-600\text{ m}, 600\text{ m})$, that is, the standard deviation of the error distribution requires $3\sigma < 600\text{ m}$ and $1\sigma < 200\text{ m}$.

After the deployment location is selected, the role of warning signs cannot be ignored. First of all, the sign should be eye-catching, and the installation location should be as close as possible to the upper part of the buoy, so that ships coming from any direction can notice and avoid in advance [12]. Secondly, the sign should be durable, not easy to deform or break, and the text and icons on it should not fade easily, and then lose its warning effect; the installation position should be stable enough to avoid falling. The anchor light is the only warning sign of the buoy at night. The brightness should meet the warning requirements, avoid other large-volume sensors, and the signal is stable. Once a fault occurs, it should be found as soon as possible and dealt with quickly.

The area around the sea buoy is open. In most cases, the signal strength is good, but there are also some areas where the signal strength is weak, or there are other signal interference, which will affect the success rate of shore station reception. Therefore, it is necessary to confirm whether the shore station receives the data smoothly, so that once the buoy has a problem, it can be observed at the first time, which is convenient for future maintenance [13].

The failure of buoys is often caused by man-made. The main reason is that the masses are curious about buoys and the awareness of public and civil facilities is not enough to protect [14]. Propaganda in this area needs to be popularized, and the people around need to know and understand the contribution of buoys to marine meteorology. The good work of buoys is helpful to their navigation planning and ship safety.

2.2 Analysis of the Errors in the Placement of Small Buoys in Offshore

The source of the buoy array launch error is the deviation from the course error caused by the automatic navigation deployment, which is described by the yaw distance, which can be called the lateral error (the direction of the route is the longitudinal direction); the second is the deviation from the target when the buoy is launched forward. The point error, described by the cast radiometer, can be called the longitudinal error; the third is the influence of wind speed and direction [15]. In order to analyze the lateral error, for the square buoy array, for a certain type of helicopter, two deployment routes are designed, as shown in the figure (Fig. 2):

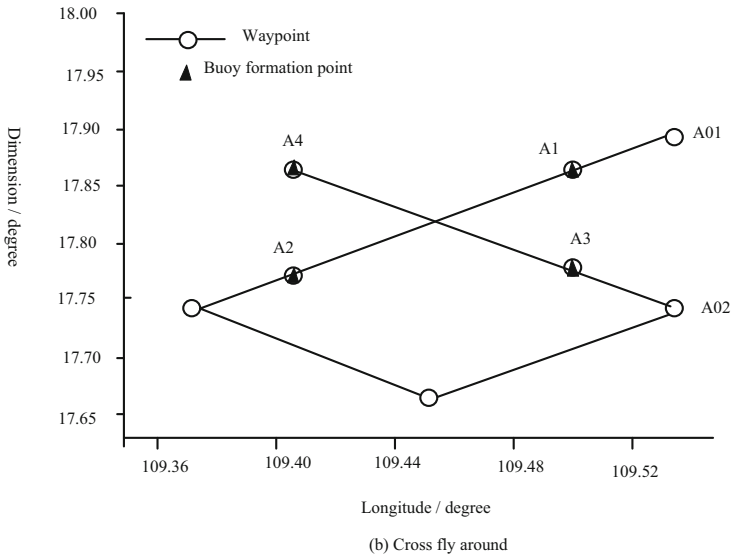
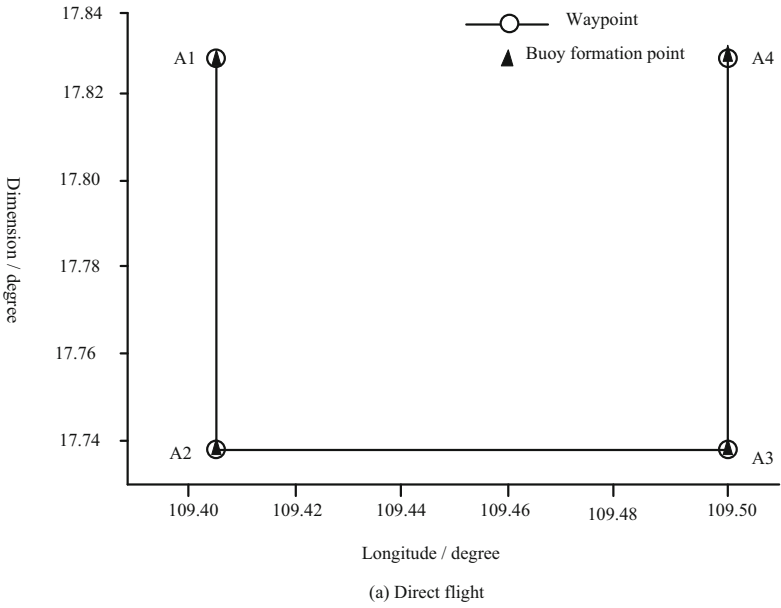


Fig. 2. Arrangement curve of square array

The trajectory of direct deployment is shown in the figure (Fig. 3).

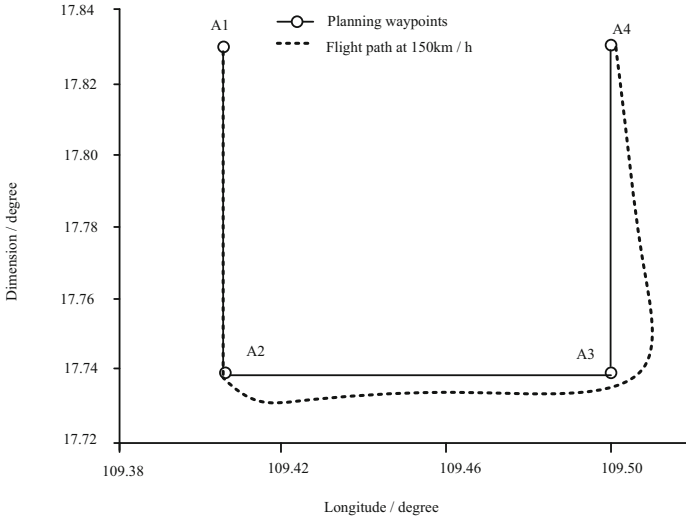


Fig. 3. Directly deploy trajectory

The yaw distance is used to describe the lateral error, and the yaw distance distribution is shown in the figure (Fig. 4).

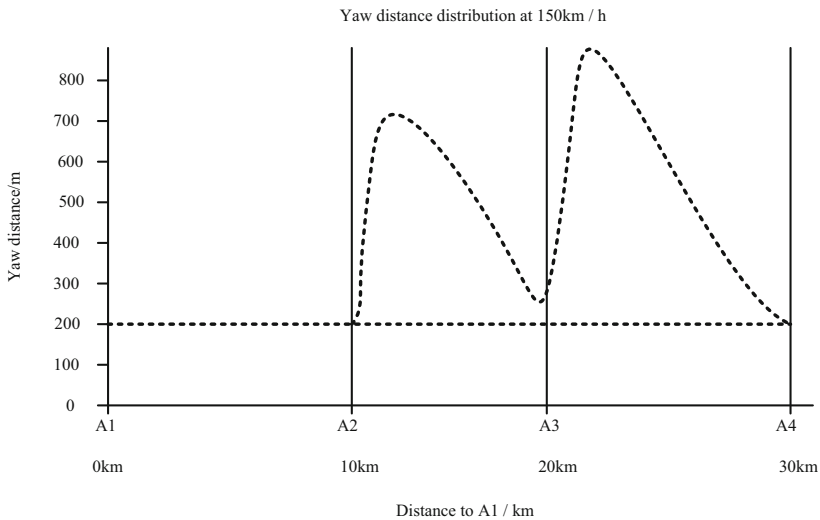


Fig. 4. Distribution of yaw distance for direct deployment

From the figure, at the turning point (A2, A3) of the square array, the yaw distance increases rapidly and then gradually converges. For a speed of 150 km/h, 10 km after

the A2 turning point, the yaw distance converges to 241 m. Deploy 10 km after the A3 turning point, and the yaw distance will converge <200 m. The A3 yaw distance exceeds the maximum deployment error requirement of the formation. The deployment trajectory of the cross-wind fly is shown in the figure (Fig. 5).

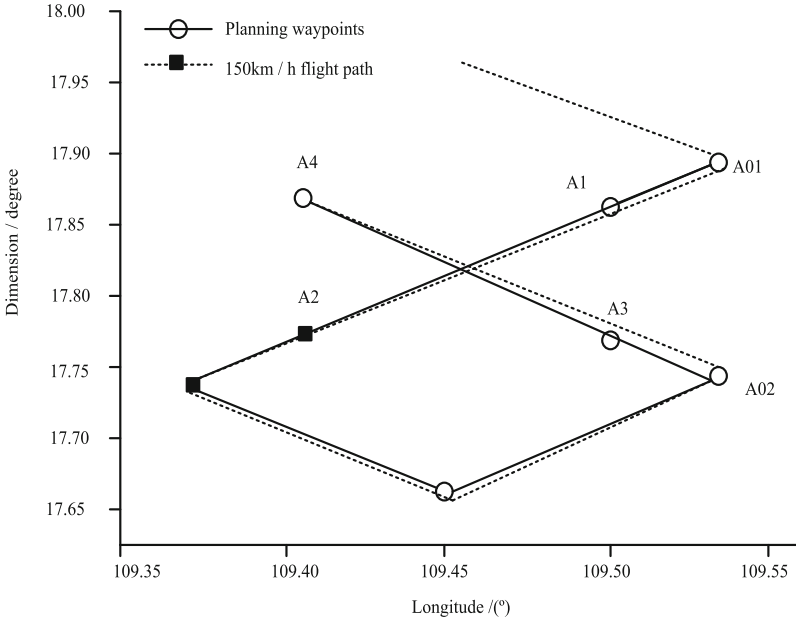


Fig. 5. Cross-wind deployment trajectory

Based on the foregoing analysis, in order to meet the requirements of the maximum launch error of the buoy formation, when designing the launch route, a route guidance point can be added before the formation route turning point, and the guidance point is more than 9 km away from the route turning point. The longitudinal error is the distance between the actual water entry point of the buoy and the planned array point when the aircraft is flying forward along the route. The longitudinal error can be controlled by calculating the buoy projection radiation table and launching according to the firing table [16]. When the influence of wind is not considered, after the buoy leaves the aircraft, it freely falls in the vertical direction, opens the umbrella and enters the water; moves at a constant speed in the horizontal direction, and opens the umbrella to slow down. The longitudinal error is the distance between the actual entry point of the buoy and the planned array point when the aircraft is flying forward along the route. The longitudinal error can be controlled by calculating the buoy emission meter and launching it according to the launch meter. When the wind influence is not considered, after the buoy leaves the aircraft, it will free fall in the vertical direction and open the umbrella into the water [17]. Perform a uniform movement in the horizontal direction and decelerate when the parachute is opened. Each time period is shown in the figure (Fig. 6):

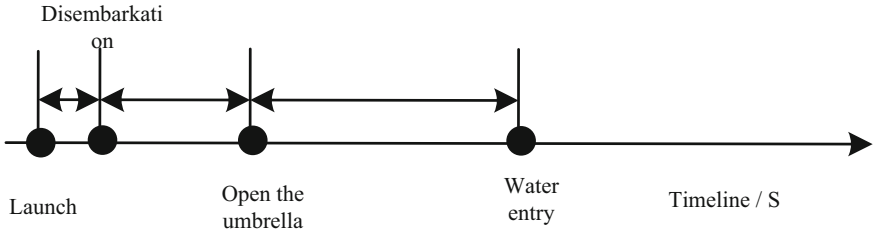


Fig. 6. Schematic of the buoy release time period

In the figure, t_0 is the time from when the release button is pressed to when the buoy leaves the machine, that is, the response lag time; t_1 is the time from when the buoy leaves the machine to when the buoy opens its parachute; t_2 is the time from when the buoy is opened to the buoy enters the water [18]. After opening the parachute, the movement model of the buoy into the water is as follows: the buoy is opened about 1s after exiting the cabin. Regardless of the influence of wind speed, the movement of the buoy is affected by the combined action of gravity G and resistance F_s , as shown in the figure (Fig. 7).

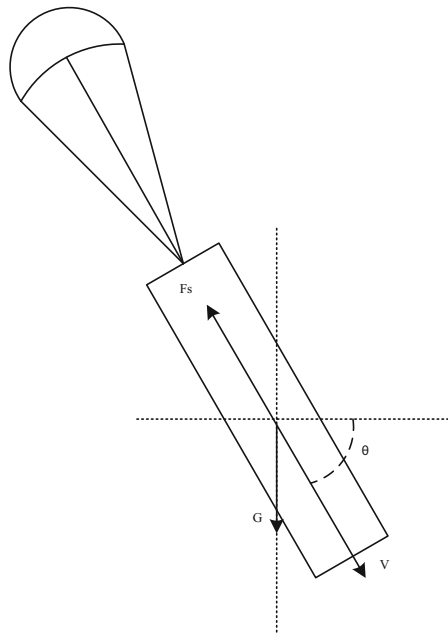


Fig. 7. Schematic of the air movement of the buoy

In the figure, F_s is resistance, G is gravity, and θ is the angle between the speed direction and the horizontal direction. After the parachute is opened, the air movement

of the buoy is represented by the following equations

$$\begin{cases} \frac{dv}{dt} = g \sin \theta - \frac{c_d S \rho v^2}{2m} \\ \frac{d\theta}{dt} = \frac{g \cos \theta}{v} \end{cases} \quad (1)$$

In the formula, v is the air movement speed of the buoy, g is the acceleration of gravity, C_d is the drag coefficient, and S is the parachute drag area. ρ is the air density, generally 1.225 kg/m³; m is the mass of the buoy. The relationship between longitudinal displacement L and height H and time T is:

$$L = v_n t_1 + \int_0^{t_2} v \cos \theta \frac{dv}{dt} \quad (2)$$

$$H = \frac{1}{2L} g t_1^2 + \int_0^{t_2} v \sin \theta dt \quad (3)$$

$$T = H(t_1 + t_2) - \frac{d\theta}{dt} \quad (4)$$

In the formula, v_n is the deployment speed of the carrier; t_1 is the parachute-opening time; g is the acceleration of gravity; t_2 is the time for the buoy to enter the water after the parachute is opened; v and θ are determined by the formula, and T is the time for the buoy to enter the water. According to the above model, the buoy shooting table under the typical launching conditions of 100 m launching height and 150 km/h launching speed is as follows (Table 2):

Table 2. Buoy projection radiation table

Launch height(m)	Water entry angle(°)	Water entry velocity(m/s)	Longitudinal displacement into water(m)	Water entry time(s)	Carrier speed(km/h)
100	87.2	17.5	97	7.4	150

The main sources of the longitudinal error σ_L are the position error σ_D of the aircraft at the time of launch, the displacement σ_{i0} produced by the response lag time error of the launch button, the displacement σ_{i1} produced by the time error of opening the parachute after the buoy is out of the cabin, the longitudinal displacement produced after the parachute is opened to the stable state of the buoy movement Error σ_s , the influence of wind σ_w . It can be obtained from each error source:

$$\sigma_L = T \sqrt{\sigma_D^2 + \sigma_{i0}^2 + \sigma_{i1}^2 + \sigma_s^2 + \sigma_w^2} \quad (5)$$

Without considering the influence of wind, the longitudinal error is:

$$\Delta\sigma_L = T \sqrt{\sigma_D^2 + \sigma_{i0}^2 + \sigma_{i1}^2 + \sigma_s^2} \quad (6)$$

Assuming the values of each parameter are: the position error of the carrier is the navigation error of the carrier, set to $\sigma_D = 30$ m; the displacement error generated by the response lag time of the launch button is $\sigma_{t0} = v_{\text{carrier}} \Delta t_0$, v_{carrier} is the carrier speed; Δt_0 is The response lag time error is set to $\Delta t_0 = 0.5$ s; the displacement error generated by the parachute opening time after the buoy leaves the cabin is $\sigma_{t1} = v_{\text{carrier}} \Delta t_1$, v_{carrier} is the carrier speed; Δt_1 is the parachute opening time error after exiting the cabin, set It is $\Delta t_1 = 1$ s; the displacement error σ_s generated after the parachute is opened to the steady state of the buoy movement is set to $\sigma_s = 20$ m. Under the above assumptions, for typical launch conditions, the longitudinal error of the buoy entering the water is 58.9 m. When the buoy is released, the longitudinal offset is controlled according to the buoy shooting table, which can realize the control of the release error. In actual deployment, in addition to the buoy shooting table, the influence of wind should also be considered. The influence of wind is the influence of wind speed and direction on the movement state t of the buoy after the parachute is opened, which leads to the deviation of the displacement of the buoy. At the time of delivery, the influence of wind can be eliminated by calculating the wind offset for real-time correction, but the error caused by the fluctuation of wind speed cannot be eliminated. Through the foregoing analysis, under different lateral error conditions, the buoy placement error is shown in the table (Table 3).

Table 3. Buoy release error

Longitudinal error(m)	Lateral error($1\sigma/m$)	Total error($1\sigma/m$)	Wind random error (m)	Accuracy requirements($1\sigma/m$)	Error margin(m)
58.9	50	77.6	7	< 200	122.4
58.9	100	116.3	7		83.7
58.9	150	161.3	7		38.7
58.9	190	199.1	7		0.9

It can be seen from the table that reducing the lateral error can make the total error meet the maximum error requirement of the buoy formation and ensure that no alarm is missed. To launch the route for the square array of buoys, increase the turning guide points to reduce the yaw distance, control the lateral error, and make the total error meet the requirements.

2.3 Optimization of the Deployment Method of Small Buoys

The offshore marine buoy body is a kind of offshore floating body, and its basic design and theoretical research refer to the general theoretical research methods of the current offshore floating body structure. In order to better analyze the structure of the offshore buoy body, the article uses the basic analysis method of panel integration based on the three-dimensional potential flow theory to focus on the basic parameters of the target

body structure that affect the buoy's motion response in the time domain and frequency domain.

When accelerating an object immersed in water, not only the object must be accelerated, but also the mass of a certain amount of water approaching the object or in front of it. The force F' required to accelerate an object in water is greater than the force F required to accelerate the same object in a vacuum. which is

$$F' = (m + m')a > F = ma \quad (7)$$

In the formula, m' is the attached mass added by attached water, and $m + m'$ is called virtual mass.

Internal analysis of the influence of these basic parameters on the force, motion performance and hydrodynamic parameters of the target body. Since the motion response of the buoy is mainly affected by the external environmental load, in order to better study the influence of the basic parameters of the target body on the motion performance of the target body, in this article, based on the analysis of the buoy body structure motion performance, we will focus on A more detailed analysis is carried out on the hydrodynamic parameters of the target body in a wave environment (Fig. 8).

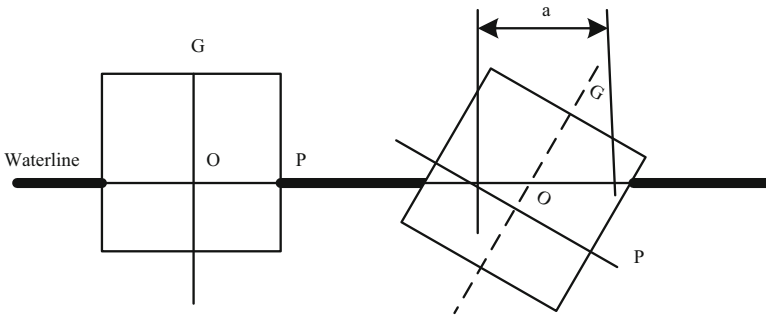


Fig. 8. Schematic diagram of static balance of floating body on water surface

When analyzing the motion performance and hydrodynamic parameters of offshore floating bodies, the offshore buoy body is usually considered as a rigid structure. The buoy body is a kind of rigid body. The marine buoy body can generally move freely in space. Therefore, when analyzing the motion performance and hydrodynamics of the marine buoy, it is necessary to establish a suitable structure for the marine buoy body under study. The coordinate system, otherwise there will be a lack of reference. For any object moving in space, its movement can be represented by six orthogonal direction vectors, as shown in the figure (Fig. 9):

The dynamic coordinate system (X', Y', Z') is established on the object, where the $X'O'Y'$ plane is established on the vertical plane of the object, and the Z axis is on the vertical $X'O'Y'$ plane and passes through the center of gravity of the object.; The fixed coordinate system (X, Y, Z) is based on a fixed reference system in space, where the XOY plane is established on the undisturbed stationary sea surface, and the Z axis is perpendicular to the sea level and upwards. For marine buoys, its movement

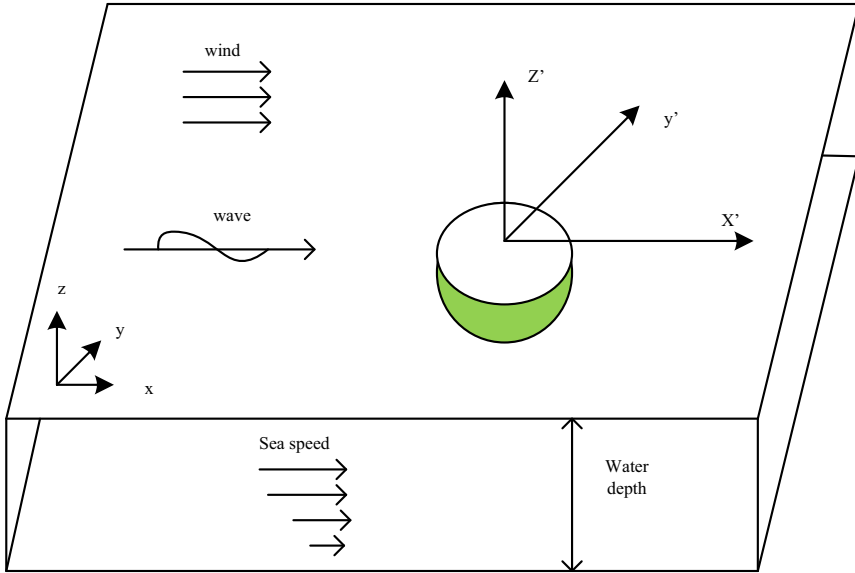


Fig. 9. The coordinate system of the rigid body movement of the buoy

in space can be described in terms of position and posture. Position is used to describe the geographic location of the marine buoy in the marine environment, including three degrees of freedom: heave, sway, and surge. Where x represents surge, Y' represents horizontal sway, z' represents heave; attitude is used to describe the appearance of marine buoys in the marine environment, such as tilt, rotation, etc., including pitch, roll, and yaw. For three degrees of freedom, the posture can be described by a posture matrix composed of the cosine values of the angles between the three coordinate axes of the coordinate system, where a_1 represents pitch, a_2 represents roll, and a_3 represents yaw. Therefore, the movement state S of the buoy can be expressed as a formula.

$$S = x'i + y'j + z'k + w \times r \tag{8}$$

$$w = \Delta\sigma_L(a_1i + a_2j + a_3k) \tag{9}$$

$$r = S(x'i + y'j + z'k) - w \tag{10}$$

The natural period is an important indicator to measure the movement performance of a floating body. Since the main floating bodies of circular buoys are symmetrical to each other, when the mounted instruments are arranged, the mounted instruments are generally arranged symmetrically. Therefore, the natural periods of the buoys in the roll and pitch directions are roughly the same. In the calculation of the natural period of the buoy, It is only necessary to consider the natural period of the rolling direction of the buoy. According to the seakeeping theory, the approximate natural frequency of the free

rolling of the floating body is:

$$f_{\theta} = \frac{1}{2\pi r} \sqrt{\frac{Dh}{J_{\theta} + \Delta J_{\omega}}} \quad (11)$$

Among them, f is the natural frequency of free rolling of the floating structure, the unit is Hz; center, is the moment of inertia of the floating body rolling motion, the unit is $\text{kg}\cdot\text{m}^2$; ΔJ_{ω} is the additional moment of inertia of the floating body rolling motion, the unit is $\text{kg}\cdot\text{m}^2$; D is the displacement, kg; h is the horizontal stability of the center height, the unit is m; the calculation formula of the natural frequency of the buoy heave is as follows

$$f_z = \frac{1}{2\pi} \sqrt{\frac{\rho g S_w}{\frac{D}{g} + m_z}} - f_{\theta} \quad (12)$$

Among them, the natural frequency of the free heave of the floating body, Hz, m_z are the additional mass of the free heave of the floating body, D is the displacement of the floating body; g is the acceleration of gravity, and the unit is m/s^2 . ρ is the density, the unit is kg/m^3 S_w is the area of the load waterline. The movement performance of the buoy is related to whether the buoy equipped instrument can normally collect marine environment information and transmit data. In order to improve the movement performance of the buoy in the marine environment, this chapter proposes to improve the buoy vertical The design of the heave plate for the oscillating motion performance and the buoy anti-rolling design based on the TMD damping theory, and the feasibility calculation and analysis of the new design. In order to increase the additional mass of the buoy in the heave freedom, based on the design of the Spar platform, it is proposed to add a heave plate to the bottom of the hemispherical small marine buoy as shown in the figure (Fig. 10).

By analyzing the calculation formula of the natural period of the buoy, it can be known that the main parameters that affect the natural period of the buoy's roll and heave motion include moment of inertia, displacement, horizontal stability center height, and load waterline area, etc., and these parameters are usually determined by the buoy structure The weight of the equipment is determined by the weight and arrangement of the equipment. Through the analysis of the above formula, it can be seen that an appropriate increase in the weight of the buoy body can appropriately reduce the natural frequency of buoy heave and appropriately increase the natural frequency of buoy roll; under the premise of an appropriate increase in the area of the load waterline, it can be effective Improve the heave natural frequency of the buoy; appropriately reducing the buoy's moment of inertia and the additional moment of inertia can increase the natural frequency of the buoy's movement and reduce its natural period.

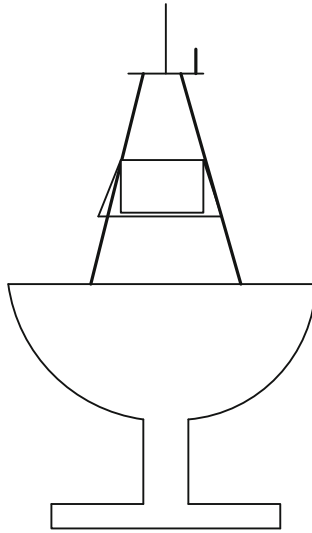


Fig. 10. Hemispherical marine buoy with heave plate

3 Analysis of Results

Two models of FVCOM and ROM were selected for this experiment. The FVCOM and ROMS models have many different sub-models. There are global and regional, climate and oceanic models, and there are many different models even in the northeastern waters of the United States.



Fig. 11. Schematic diagram of sea trial

The buoy was transported to the Dalian Zhangzidao Wharf, where the temperature chain and the steel cable were connected and the anchoring was installed on the shore. Under the command and strong assistance of the marine technology research and development department of the Zhangzidao Fishery Group and the crew on the experimental ship, the overall installation went smoothly (Fig. 11).

The main purpose of this experiment is to compare and study various situations of drifting buoys at different depths, and to compare their influences. Since the result of each experiment is the latitude and longitude of each time point of the model or drifting buoy, it is necessary to convert the difference in latitude and longitude into a distance difference. This experiment uses the following formula:

$$a = \sin\left(\frac{(\text{lat}2 - \text{lat}1)}{2}\right)^2 + \cos(\text{lat}1) \times \cos(\text{lat}2) \times \sin\left(\frac{(\text{lon}2 - \text{lon}1)}{2}\right)^2 \quad (13)$$

At the same time, when calculating the daily average error distance, the hourly distance error data is divided by the time weight, that is, the hourly distance error data is divided by 24th of the elapsed time. Every hour will get the error data of one kilometer per day, and divide this data by 24 to get the real error data for another day. Seawater can be divided into many layers in the horizontal direction, and the flow direction and speed of the seawater between different layers are different. It is not possible to simply replace the operation of the entire ocean current with one layer of ocean current. But in order to be able to better carry out the digital representation, but also for more convenient research, in many cases the sea water will be divided into multiple layers, the specific number of layers depends on the situation. This experiment uses drifting buoys to study different levels of sea and ocean currents. There are three types of buoys used, one is a four-rectangular page fan on the surface, and the other is a bucket-shaped submarine mark, as shown in the figure (Figs. 12, 13, 14, 15).

The heave and pitch motion RAOs of the hemispherical, truncated cone-shaped and cylindrical floating body models under ballast are obtained by numerical simulation.

The buoy is still in the testing state. The first step of the experiment is to filter the data. Choose a pair of buoys with a starting time interval of less than 1 h, a distance of less than 1 km and different depths, and compare the first three pairs of drifting buoys. Days of data. The data after three days is no longer of experimental significance and value because of the relatively large interval. Comparing the results of the experimental data, it is found that the results of the movement of the buoys at different depths under different conditions are different. Some directions are basically the same, while some are far apart, and some are more consistent at the beginning but inconsistent later. Comparing the data of this experiment, it is found that there are many errors. The first is the influence of the experimental data caused by the different styles of the drifting buoys on the upper and lower layers and the different responses after being stressed. Secondly, submersible targets often cross multiple water layers. Even if the buoy is small, the floating objects on the water and the line connecting the floating objects and the buoy will affect the movement of the submersible. Moreover, in order to achieve the production parameters of the submersible, the buoy itself It is not very small, and the direction of ocean currents between different water layers is not completely consistent, so this will inevitably affect the data results. In addition, it also includes the impossibility of placing buoys at exactly

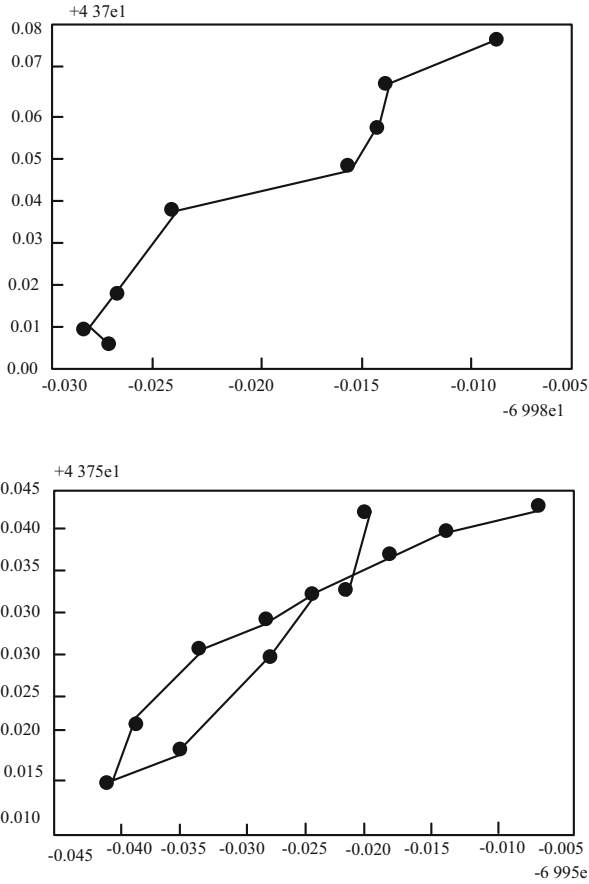


Fig. 12. Detection results of buoys at different depths

the same time and place. In addition to these errors, the data will also have various completely different problems. The red trajectory of the two trajectories on the left has only six data, which is probably caused by the damage of the buoy, which leads to the damage of the positioning system or the inability to send a signal for other reasons. And some data are extremely similar to the reason that the buoy is damaged, and the connection between the main body of the submersible target and the floating object storing the positioning system is disconnected, which causes the submersible target to become a kind of surface drifting buoy. The two types of drifting buoys are surface drifting buoys, so even if the styles are different, the data after running are very similar. Some similarities are caused by the similarity of ocean currents on the surface layer and the layer where the potential target is located. However, because the damage of the buoy cannot be determined in time, the real reason for the similar trajectory cannot be determined.

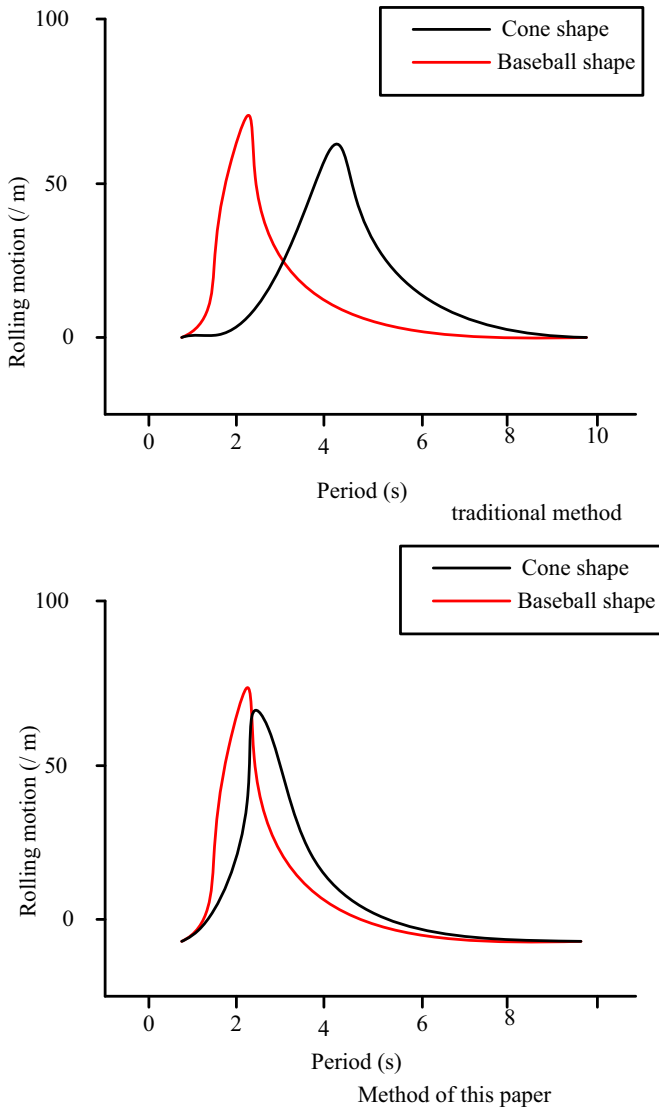


Fig. 13. Comparison results of roll motion response

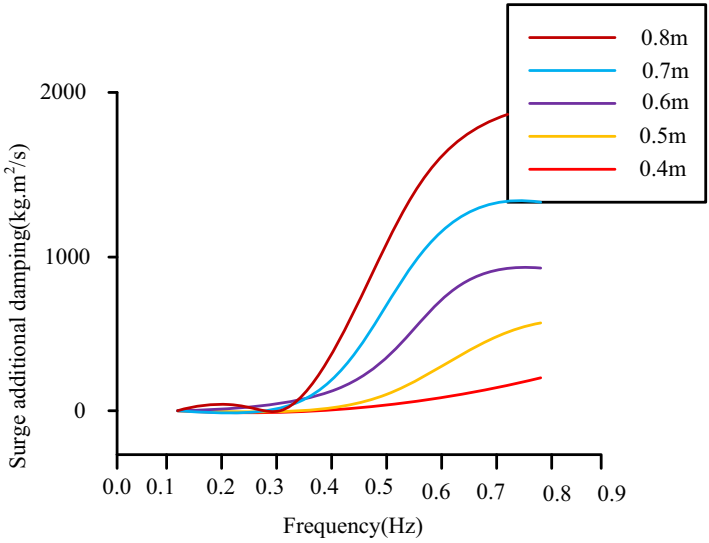


Fig. 14. The effect of draft on the additional damping of turbulence

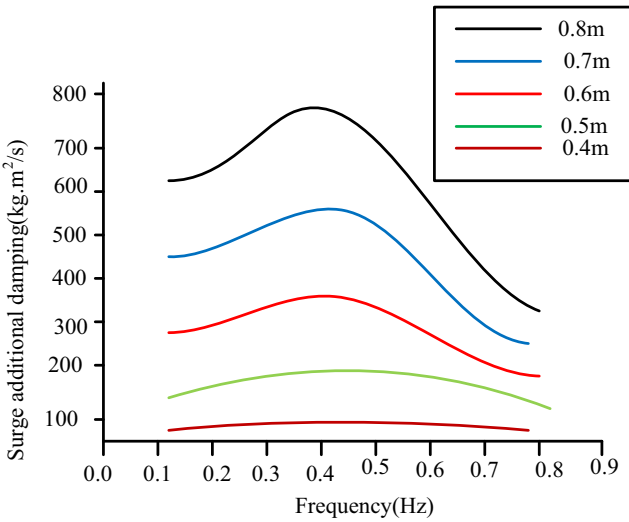


Fig. 15. The effect of draft on the additional mass of sloshing

4 Concluding Remarks

At this stage, the deployment conditions of small offshore buoys in China are relatively unfavourable, but if all parties can fully prepare and cooperate, the whole process can be orderly, safe and smooth. Buoy array anti-submarine is an important means of aviation anti-submarine. Controlling the accuracy of buoy placement is an effective measure to improve the anti-submarine efficiency of the buoy array. Planning the buoy placement

route is the key to achieving high-precision buoy placement. The purpose of planning the buoy array route is to select a reasonable route that meets the performance index requirements of the buoy array and satisfies the aircraft deployment performance. At present, the research on the sonar buoy deployment formation simulation to improve the search probability of the buoy array is mainly carried out in this field in China. There is no report about the research on the influence of the buoy deployment error on the submarine search efficiency of the formation. In practical engineering applications, we found that the impact of buoy placement errors on the effectiveness of the buoy array cannot be ignored. Excessive placement error may lead to a decrease in the effectiveness of the formation's search for submarine, and even a large gap in the formation, resulting in missed alarms. From the perspective of engineering practice, this paper proposes a route experiment and error analysis method to reduce the error of the buoy array, which can achieve the purpose of effectively controlling the error of the buoy array.

References

1. Roostaei, J., Colley, S., Mulhern, R., et al.: Predicting the risk of GenX contamination in private well water using a machine-learned Bayesian network model. *J. Hazardous Mater.* **411**(10), 125075 (2021)
2. Ruggieri, A., Stranieri, F., Stella, F., et al.: Hard and soft EM in Bayesian network learning from incomplete data. *Algorithms* **13**(12), 329 (2020)
3. Zhao, C., Cao, F., Shi, H.: Optimisation of heaving buoy wave energy converter using a combined numerical model. *Appl. Ocean Res.* **102**(11), 102208 (2020)
4. Yang, J., Zhang, J.: Validation of Sentinel-3A/3B satellite altimetry wave heights with buoy and Jason-3 data. *Sensors* **19**(13), 2914 (2019)
5. Sheridan, L.M., Krishnamurthy, R., Gorton, A.M., et al.: Validation of reanalysis-based offshore wind resource characterization using Lidar buoy observations. *Mar. Technol. Soc. J.* **54**(6), 44–61 (2020)
6. Venkatesan, R., Ramesh, K., Muthiah, M.A., et al.: Estimation of uncertainty in the atmospheric pressure measurement from the Indian ocean moored buoy systems. *Mar. Technol. Soc. J.* **55**(1), 137–146 (2021)
7. Meng, L., Wu, R., et al.: Experimental study on conversion efficiency of a floating OWC pentagonal backward bent duct buoy wave energy converter. *China Ocean Eng.* **33**(03), 50–61 (2019)
8. Mcallister, M.L., Van, D.: Lagrangian measurement of steep directionally spread ocean waves: second-order motion of a wave-following measurement buoy. *J. Phys. Oceanogr.* **49**(12), 3087–3108 (2019)
9. Venkatesan, R., Sannasiraj, S.A., Ramanamurthy, M.V., et al.: Development and performance validation of a cylindrical buoy for deep-ocean tsunami monitoring. *IEEE J. Oceanic Eng.* **44**(2), 415–423 (2019)
10. Yurovsky, Y., Dulov, V.A.: MEMS-based wave buoy: towards short wind-wave sensing. *Ocean Eng.* **217**(10), 108043 (2020)
11. Nielsen, U.D., Dietz, J.: Estimation of sea state parameters by the wave buoy analogy with comparisons to third generation spectral wave models. *Ocean Eng.* **216**(9), 107781 (2020)
12. Zhang, H., Zhou, B., Vogel, C., et al.: Hydrodynamic performance of a floating breakwater as an oscillating-buoy type wave energy converter. *Appl. Energy* **257**(8), 113996–113999 (2020)

13. Oikonomou, C., Rui, P., Gato, L.: Unveiling the potential of using a spar-buoy oscillating-water-column wave energy converter for low-power stand-alone applications. *Appl. Energy* **292**(11), 116835 (2021)
14. Zhang, H., Zhou, B., Vogel, C., Willden, R., Zang, J., Geng, J.: Hydrodynamic performance of a dual-floater hybrid system combining a floating breakwater and an oscillating-buoy type wave energy converter. *Appl. Energy* **259**, 114212 (2020)
15. Palm, J., Eskilsson, C.: Mooring systems with submerged buoys: influence of buoy geometry and modelling fidelity. *Appl. Ocean Res.* **102**, 102302 (2020)
16. Kumar, S., Nagababu, G., Kumar, R.: Comparative study of offshore winds and wind energy production derived from multiple scatterometers and met buoys. *Energy* **185**, 599–611 (2019)
17. Li, J., Huang, H., Chen, X., et al.: The small-signal stability of offshore wind power transmission inspired by particle swarm optimization. *Complexity* **2020**(13), 1–13 (2020)
18. Cao, Z., Liu, J., Lin, Z., et al.: Effects of inclined condition on LOCA for a small offshore reactor with OTSG. *Nuclear Eng. Des.* **375**(4), 111098 (2021)